Tensor-based Detection of Paroxysmal and Persistent Atrial Fibrillation from Multi-channel ECG

Moghaddasi, H.; Veen, A.J. van der; Groot, N.M.S. de; Hunyadi, B.

Publication date
2020

Document Version
Final published version

Published in
28th European Signal Processing Conference (EUSIPCO 2020)

Tensor-based Detection of Paroxysmal and Persistent Atrial Fibrillation from Multi-channel ECG

Hanie Moghaddasi
Circuits and Systems Group
Delft University of Technology
Delft, Netherlands
H.Moghaddasi@tudelft.nl

Alle-Jan van der Veen
Circuits and Systems Group
Delft University of Technology
Delft, Netherlands
A.j.vanderveen@tudelft.nl

Natasja M.S. de Groot
Department of Cardiology
Erasmus University Medical Center
Rotterdam, Netherlands
N.m.s.degroot@erasmusmc.nl

Borbála Hunyadi
Circuits and Systems Group
Delft University of Technology
Delft, Netherlands
B.Hunyadi@tudelft.nl

***Abstract*—Atrial fibrillation (AF) is the most common arrhythmia in the heart. Two main types of AF are defined as paroxysmal and persistent. In this paper, we present a method to discriminate between the characteristics of paroxysmal and persistent using tensor decompositions of a multi-channel electrocardiogram (ECG) signal. For this purpose, ECG signals are segmented by applying a Hilbert transform on the thresholded signal. Dynamic time warping is used to align the separated segments of each channel and then a tensor is constructed with three dimensions as time, heartbeats and channels. A Canonical polyadic decomposition with rank 2 is computed from this tensor and the resulting loading vectors describe the characteristics of paroxysmal and persistent AF in these three dimensions. The time loading vector reveals the pattern of a single P wave or abnormal AF patterns. The heartbeat loading vector shows whether the pattern is present or absent in a specific beat. The results can be used to distinguish between the patterns in paroxysmal AF and persistent AF.**

Keywords—Atrial fibrillation, Tensor decomposition, Electrocardiogram and Canonical polyadic decomposition

I. INTRODUCTION

Atrial Fibrillation (AF) is the most prevalent sustained arrhythmia in the heart and can lead to stroke, heart failure and other heart-related diseases [1]. In a normal person, the electrical activity of the heart starts from the sinoatrial (SA) node and propagates to the atrioventricular (AV) node which creates regular beats. However, in AF, impulses from other sites in the atrium generate irregular beats which change the signal morphology as well as the heart rate. The clearest feature of AF in an electrocardiogram (ECG) is the irregular R-R interval during the AF episode. There are two main types of AF: paroxysmal and persistent. In paroxysmal AF, irregular beats start suddenly and the heart rhythm goes back to the normal rhythm by itself. Episodes of AF occur occasionally and last between 30 seconds and 7 days. Besides, atrial premature beats (APB) also can lead to paroxysmal AF. APB happens when a site in the atrium depolarizes before SA node and subsequently triggers a heartbeat. Wallmann et al. [2] derived that frequent APB can lead to AF. They defined that if the number of APB is higher than 70 in 24 hours, the probability of AF increases by 28% in stroke patients. In persistent AF, the irregular beats last more than 7 days and do not terminate by themselves. In both paroxysmal AF (AF episode) and persistent AF, instead of a single P wave, fibrillatory waves or absence of P wave are recorded in the ECG signal. However, this classification is not always very practical or insightful as one would have to measure for 7 days, and it does not describe the severity. This motivates to search for a different classification.

Currently, AF diagnosis is based on the surface ECG and Holter monitoring. In previous works, only the AF episodes of an ECG signal are selected for the classification. However, between 25% and 60% of AF cases are paroxysmal AF, which have both AF episodes and NSR episodes in the recorded ECG signal. Moreover, most automatic detection methods work on a single channel ECG [3]. A multi-channel ECG has spatiotemporal information which is helpful in the AF analysis.

In this paper, we present a novel method to define and detect characteristic patterns in paroxysmal AF and persistent AF in a multi-channel ECG. A multi-channel ECG consists of temporal information from different heartbeats and different channels. After segmentation, we stack this information in a tensor (high dimensional matrix). A tensor decomposition factors the tensor into lower-dimensional components (loading vectors), which approximate the original tensor. Tensor has been widely used in various cardiac applications. Detection and localization of myocardial infarction (MI) [4], ECG data compression [5], irregular heartbeat classification [6], and detection of T-wave alternans [7] are examples of these researches in cardiology. Previously, Giernaert et al. [8] proposed using a multilinear singular value decomposition (MLSVD) for the classification of short periods of ECG signals into AF or NSR. However, both episodes are present when we analyze longer periods, as is necessary for detecting paroxysmal AF. If an algorithm or physician only looks at the NSR segment of the signal, the AF would not be detected.

Therefore, we concentrate on long-duration AF patient data and propose a tensor-based method to extract characteristics of paroxysmal AF and persistent AF. The advantage of our work is that the proposed method is able to compress a very long ECG signal into three loading vectors, which can also reveal the short episodes of AF. Moreover, the tensor analysis shows that each class of AF (paroxysmal, persistent) can be further decomposed into two sub-groups (type A, type B), which represent discriminant features of paroxysmal AF and persistent AF. The loading vector also allows us to estimate (and generalize) the AF burden, which is a widely used parameter to assess the severity of AF.

This research was funded in part by the Medical Delta Cardiac Arrhythmia Lab (CAL).

II. METHOD

A. Data

We used ECG telemetry data, collected at Erasmus Medical Center (EMC) from 13 patients, 6 with paroxysmal AF and 7 with persistent AF. The data are standard 12-lead ECG signals which last 72 hours and are labeled by clinicians as paroxysmal AF or persistent AF. All ECG signals are recorded with a sampling frequency 200 Hz. As telemetry recording is a time-consuming process and leads are connected to patient for days, artifacts are highly possible on the recorded data, especially on the body leads. Hence, we excluded body leads' data and studied only the six chest leads' data (V_1-V_6).

Moreover, power-line, electrode connection, breathing artifact and electromyography interference are other sources of noise in ECG. Hence, a band-pass filter with a cutoff frequency of 0.33 Hz to 30 Hz is applied on all six channels. Next, the signals are also normalized in amplitude to have values between -1 and +1. The resulting signal is denoted by s_n.

B. Segmentation

The ECG of a normal heartbeat consists of three main segments the P wave, QRS complex and T wave. The P wave represents atrial depolarization during a cardiac cycle and analyzing this part will help us to study atrial activity. However, during AF, rapid fibrillatory waves of atrial activity or absence of P wave are recorded instead of the P wave. Hence, we segmented the ECG signal from the end of the T-wave (T_{end}) to the start of the QRS complex (QRS $_{start}$) [9] to concentrate on the most important part of the ECG signal from AF point of view.

In this work, we applied a Hilbert transform (HT) for the segmentation of the ECG signal. The use of HT in ECG analysis was first presented by Bolton and Westphal [10]. Benitez et al. [11] used a Hilbert transform of the first differential of the ECG to locate the R peak in the QRS complex. Varghees and Ramachandran [12] showed that a HT is useful to detect the boundaries of the local waves in the signal. They proposed a HT for heart sound activity detection and we implemented the same pre-processing steps to detect the boundaries of the local waves in the ECG signal.

Since we aim to find the boundaries of the local waves with high amplitude (T wave and QRS complex), we set an adaptive threshold based on the standard deviation σ_{s_n} of the normalized signal s_n (suppressing P wave and fibrillatory waves in the segmentation). Hence, the thresholded signal is computed as

$$s_{th}[n] = \begin{cases} 0, & s_n[n] < \sigma_{th} \\ s_n[n], & \text{otherwise.} \end{cases} \quad (1)$$

After analyzing an arbitrary short segment of each patient, we set $\sigma_{th} = 0.2 \times \sigma_{s_n}$.

Let $\hat{s}_{th}[n]$ be the HT of $s_{th}[n]$, then the analytical signal representation of the thresholded signal is computed as

$$s_a[n] = s_{th}[n] + j\hat{s}_{th}[n] = A[n]e^{i\varphi[n]} \quad (2)$$

where $s_a[n]$ denotes the analytical signal of the thresholded signal, $A[n]$and $\varphi[n]$ are the amplitude and the instantaneous phase which are computed as

$$A[n] = \sqrt{s_{th}[n]^2 + \hat{s}_{th}[n]^2}$$
$$\varphi[n] = tan^{-1}\left(\frac{\hat{s}_{th}[n]}{s_{th}[n]}\right) \quad (3)$$

For the signal $s_{th}[n]$ with zero-valued samples and positive-valued HT samples, the phase angle is $+\frac{\pi}{2}$ radian. For negative-valued HT samples with zero-valued samples, the phase angle is $-\frac{\pi}{2}$. According to (3), the negative to positive angle change appears at the peak point of the thresholded signal. So, in the instantaneous phase waveform, the zero-crossing point is determined by checking the sign of the samples at time *n* and *n+1*. Hence, the detected zero-crossing points in the phase angle represent the location of the R peak and the T peak. In the next step, peak locations are sorted into two groups as R peaks and T peaks. By analyzing all data, a threshold *c* is defined as

$$c = 0.75 \times \max(s_{th}[n]) \quad (4)$$

If $s_{th}[n]$ at $n=n_{peak1}$ is higher than *c*, n_{peak1} is the location of an R peak, otherwise, it would be the location of a T peak. The constant 0.75 was determined empirically based on a subset of the ECG data, and it is considered to be able to detect the varying-amplitude R peaks in the ECG sequence.

According to the instantaneous phase of the analytical signal, the boundaries of the local waves in the ECG signal are determined by the positive-slope line. As shown in Figure 1, the QRS complex and T wave start from $-\frac{\pi}{2}$ radian and end at $+\frac{\pi}{2}$ radian.Thus, the starting point of the positive slope is determined by checking the amplitude of the phase in samples from n_{Rpeak} backward. The first location for which the amplitude of the phase is $-\frac{\pi}{2}$ is declared as the starting point of the QRS complex. Similarly, the end point of the positive slope is determined by checking the amplitude of the phase in samples from n_{Rpeak} onwards. The first location for which the amplitude of the phase is $+\frac{\pi}{2}$ is declared as the end point of the QRS complex. This algorithm repeats for each T wave and it starts from the sample of the T peak location.

Based on the results, we observed that the detected boundaries of local waves slightly differ from the true boundaries. This error is due to the use of the threshold for low amplitude signals. The duration of the boundary location error is approximately 20 ms. So, we considered a 10 ms time delay after the T_{end} and 10 ms before QRS $_{start}$ to correct the time-location error. We repeated the proposed method for all channels. As a result, the ECG signal in the T_{end} - QRS $_{start}$ intervals has been segmented for each channel, and they are stored for further analysis.

C. Dynamic time warping

A normal heart rate is not entirely constant as cardiac cycles have slightly different lengths. This situation intensifies in

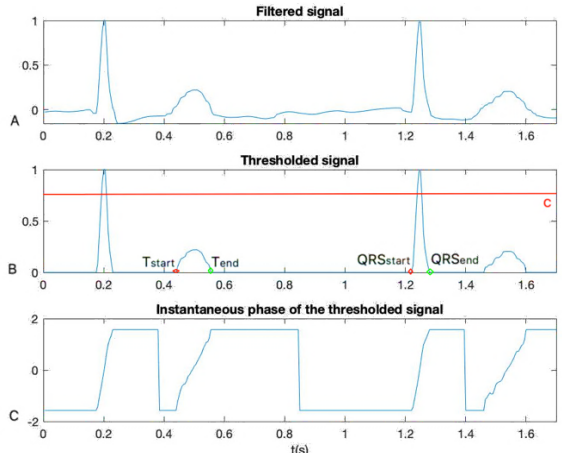

Figure 1.Segmentation of the ECG signal, A) Filtered signal B) Thresholded signal C) Instantaneous phase of the signal

cardiac arrythmia which has uneven cardiac cycles. Hence, the segmented ECG signals in all heartbeats of a single channel do not have the same length. Thus, we used dynamic time warping (DTW) to align two segmented ECG signals which correspond to two heartbeats onto a common set of samples. The DTW algorithm is applied based on the dynamic programming techniques explained in [13]. The goal of DTW is to minimize the distance between two sequences of data. Hence, it searches for an alignment path that minimizes the total cost of alignment.

In the channel one, the DTW distance is calculated between all segments. The DTW distance matrix shows that there are two groups of segments in the recorded signals based on the measured distance. Thus, in order to minimize the DTW distance, we define the mean value of the DTW distance matrix as a threshold and divide segments into two classes. In the next step, the alignment method is repeated for each class, separately. As a result, we gained aligned ECG segments from channel one with the same length. Then we aligned a segment of the channel two with the aligned segments of channel one and repeat the algorithm for other beats of channel two. The algorithm is repeated for other channels, similarly. As a result, we have aligned segments with the same length in all beats and all channels.

D. Tensor construction

A tensor is a generalization of a matrix to higher dimensions. While a single channel ECG can be stored in a vector (one dimension), the segmented ECG can be stored in a matrix (two dimensions). More specifically, if the length of $T_{end} - QRS_{start}$ segment is L and the number of heartbeats in a single-channel is M, we can create a matrix of size $L \times M$ in which each row shows a heartbeat and each column shows the time. The same is done for other channels and the resulting matrices are stacked behind each other to construct a third-order tensor with three dimensions as: *time* × *heartbeat* × *channel*. Construction of the third-order tensor $\mathcal{X} \in \mathrm{R}^{L \times M \times V}$ is shown in Figure 2 where $V = [V_1, \ldots, V_6]$ shows the number of channels.

E. Tensor decomposition

In the ECG signal, there are normal heartbeats and AF episodes. Here we assumed that the normal heartbeats are characterized by a certain temporal pattern which is present with different amplitude on different heartbeats and different channels. Further, during AF episodes, it is assumed that a different pattern is present, which is scaled in different heartbeats and channels. So, the tensor $\mathcal{X}$ can be approximated by a canonical polyadic decomposition (CPD) where each rank 1 component describes one pattern [14]. The first loading vector describes the time course of the pattern, while the second and third loading vector shows how this pattern is scaled over the beats and channels. The CPD is defined as

$$\mathcal{X} = \sum_{r=1}^{R} a_r \circ b_r \circ c_r + E \qquad (5)$$

where (a_r, b_r, c_r) are the loading vectors of component r and "$\circ$" denotes the outer product. The CPD approximates a tensor into a sum of R rank-1 components. The rank of the tensor is determined by the smallest R for which E=0 (Figure 2).

An important issue for the CPD is its uniqueness. Define first, second and third factor matrices of a third-order tensor $\mathcal{X}$ as $\mathbf{A}$=[a$_1$,…,a$_R$], $\mathbf{B}$=[b$_1$,…,b$_R$], and $\mathbf{C}$=[c$_1$,…,c$_R$]. The CPD is also written as $\mathcal{X} = [\boldsymbol{A}, \boldsymbol{B}, \boldsymbol{C}]_R$. Then, the CPD is unique if $\mathcal{X} = [\boldsymbol{A}, \boldsymbol{B}, \boldsymbol{C}]_R = [\overline{\boldsymbol{A}}, \overline{\boldsymbol{B}}, \overline{\boldsymbol{C}}]_R$ implies that an $R \times R$ permutation matrix $\boldsymbol{\Pi}$ and nonsingular diagonal matrices $\boldsymbol{\Lambda_A}, \boldsymbol{\Lambda_B}$ and $\boldsymbol{\Lambda_C}$ exist such that

$$\overline{\boldsymbol{A}} = \boldsymbol{A\Pi\Lambda_A}\ , \overline{\boldsymbol{B}} = \boldsymbol{B\Pi\Lambda_B},\ \ \overline{\boldsymbol{C}} = \boldsymbol{C\Pi\Lambda_C}, \boldsymbol{\Lambda_A\Lambda_B\Lambda_C} = \boldsymbol{I_R} \qquad (6)$$

Conditions for uniqueness of the CPD were derived by Kruskal [15] for third-order tensors and Sidiropoulos and Bro [16] for higher-order tensors. A sufficient condition for uniqueness is that A and B are full rank and C does not contain collinear columns. For small R this is satisfied to an acceptable extent.

III. RESULTS

In the CPD model, firstly the number of extracted components should be determined. In order to find the correct R, we decomposed the tensor into the different number of components and calculated the residual error by comparing the reconstructed tensor to the original tensor $\mathcal{X}$. Then the relative error is computed by dividing the Frobenius norm of residual error to the Frobenius norm of the original tensor. The relative error for a patient with paroxysmal AF and a patient with persistent AF is shown in Figure 3. For both patients, the

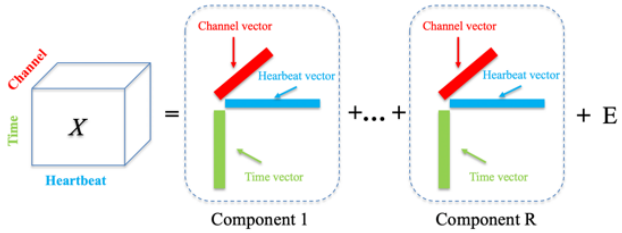

Figure 2. Tensor construction and CPD decomposition

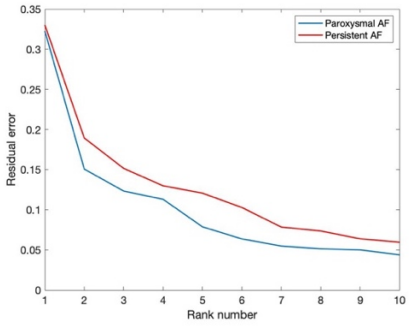

Figure 3. Relative error of tensor decomposition with different ranks

maximum error reduction happened when the rank was increased from 1 to 2 which means rank 1 is able to extract the dominant component of the signal. However, rank 1 is too small because from prior knowledge about AF in both groups, we expect to see two different patterns in each group of AF. Therefore, rank 2 is chosen to extract the patterns. Next, we study paroxysmal and persistent AF datasets and present two examples for each class.

A. Paroxysmal AF

Figure 4 shows the CPD components for two patients with paroxysmal AF. Column one shows the first loading vector which represents a template for T_{end} -QRS $_{start}$ segment. Column two shows the variation of the loading vector one in the different heartbeats. Note that the algorithm was applied to the whole telemetry data but in Figure 4 and Figure 5, we showed 100 beats. The third loading vector corresponds to the relative strength (and polarity) of the extracted pattern (first loading vector) across channels. For paroxysmal AF, we observed two distinct patterns which we call type A and type B.

Figure 4.A shows an example of type A. Looking at the first loading vector, component one (in blue) is recognized as a single P wave contributed by the NSR part, while component two (in red) is a template for fibrillatory waves. The second loading vectors show the magnitude of the extracted patterns across beats. From beat number 48, the magnitude of component two is increasing which shows the starting point of fibrillatory waves. Fibrillatory waves continue until beat number 92, after which normal sinus rhythm is restored. This can also be derived from the magnitude of component one in the second loading vector. The second loading vector is also useful to find the AF burden. From this vector the duration of AF episodes, number of AF episodes and the percentage of time that the patient is in AF can be monitored.

Figure 4.B shows the components for an example of type B. Component one (in blue) of the first loading vector shows a single P wave while component two (in red) illustrates a pattern for the absence of a P wave which is related to atrial premature beats. By analyzing the second loading vector, it is clear that the magnitude of component one is mostly higher than component two which is close to zero except for three heartbeats. In beat number 10, 25 and 72, the magnitude of component two is higher than component one, which is close to zero. This means that in these 3 beats the normal P-wave (first

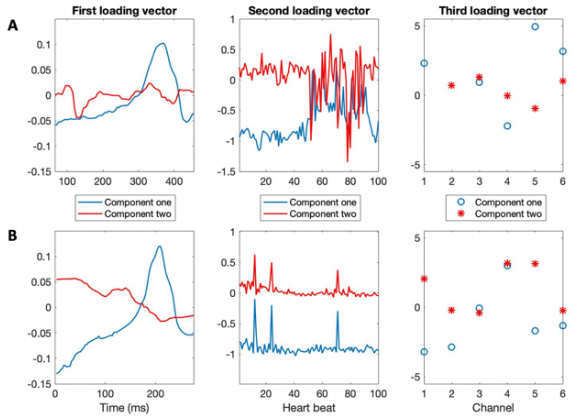

Figure 4. CPD loading vectors for two paroxysmal cases, A) type A B) type B

loading vector of the second component) is absent. By counting the number of atrial premature beats as explained in the Introduction section, a total of 138 atrial premature beats could be detected in a total length of 24 hours. So, this case shows the patterns of type B in paroxysmal AF.

In the dataset, two patients have patterns of type A and four patients have patterns of type B.

B. Persistent AF

Figure 5 shows the CPD components of two patients with persistent AF. As described in the Introduction, fibrillatory waves or the absence of a P wave are indicators of persistent AF. We observed two distinct patterns of persistent AF which we also call type A and type B (they are not related to the previous A and B).

In Figure 5.A, patterns of type A are observed. The first loading vector shows two components. Component one is a template of fibrillatory waves and component two is a template for the absence of P wave. The second loading vector gives information about the distribution of fibrillatory waves as well as the absence of P wave. By analyzing two components of the second loading vector, it is determined that most beats represent the pattern of the fibrillatory wave while some beats, like beat number 54, have an absence of a P wave.

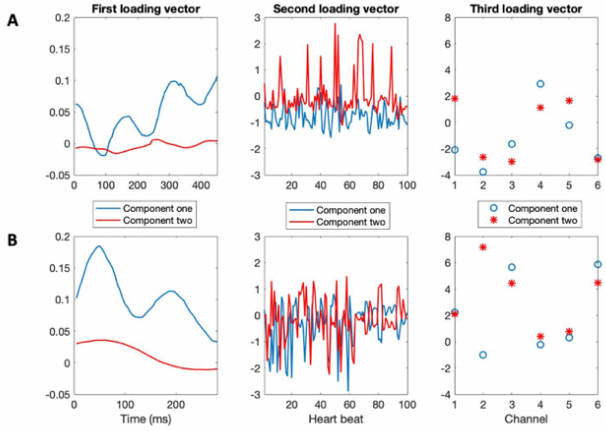

Figure 5. CPD loading vectors of in two persistent cases, A) type A B) type B

In case two, fibrillatory waves and the absence of a P wave are shown as components of the first loading vector, similarly. The difference between type A and type B is in the distribution of components. In type B, the number of beats with a fibrillatory pattern are almost the same as the beats with the absence of a P wave pattern. These features are considered as patterns of type B in persistent AF. In other words, the most discriminant feature of type A and type B is the percentage of fibrillatory waves compared to the absence of P waves. For type B, the percentage of fibrillatory waves is higher than for type A, and this feature can be used to assess the severity of persistent AF. For further analysis of such a severity estimation, we have to observe more data. In the dataset, three patients have patterns of type A and four patients have patterns of type B.

IV. DISCUSSION

In this work, we present a novel method to find specific patterns in multichannel ECGs to reveal differences between paroxysmal AF and persistent AF. The most important difference between these conditions is the fact that in paroxysmal AF, NSR (including P-waves) and AF episodes (without P-waves) are alternating, while in the persistent AF, NSR (i.e. P-waves) is almost absent. This difference can only be established using long ECG recordings. Reading long-term multichannel ECG is time-consuming and cumbersome. Our approach provides a compact and easy-to-interpret summary of all the patterns present in the ECG in just 3 figures that visualize the loading vectors: the most prevalent patterns, their presence in the consecutive waves and their relative strength in the different channels. Paroxysmal and persistent AF can be differentiated directly from the first loading vector, based on the presence or absence of a loading vector resembling a P-wave pattern.

It is important to note that while the proposed method is able to distinguish between persistent AF and paroxysmal AF, in borderline cases an improvement in the method is needed. For example, if the AF episodes in a paroxysmal case lasts slightly less than 7 days, the NSR episode would be too short. So, it is possible that the pattern of a single P wave is not extracted by the rank 2 CPD. Also, atrial activity can be modeled by the sum of complex exponentials and the block term decomposition (BTD) exploits this signal model to apply source separation. Thus, based on the signal model, using BTD can be helpful in the detection of borderline cases [17].

Moreover, the second loading vector of the CPD can also be useful in the severity detection of AF. This vector shows the distribution of a single P wave, absence of P wave and fibrillatory waves. Hence, by analyzing the second loading vector of a large group of the graded data we can find the relationship between the extracted patterns and the severity of AF.

V. CONCLUSION

This paper presents a tensor-based method to extract characteristics of paroxysmal and persistent AF in the multi-channel ECG signals. Results of patients in both groups reveal that CPD is able to find components that illustrate the distinction between paroxysmal and persistent. Our future work is to improve the proposed method for borderline cases and apply this method to a larger dataset to classify them automatically. Having more information about AF will lead to the improvement of AF treatment. Hence, we aim to extend this method to find the relationship between the extracted components and the severity of AF. This can be also helpful for the treatment of patients in the early stages.

VI. REFERENCES

[1] Lloyd-Jones, D.M., et al., *Lifetime risk for development of atrial fibrillation: the Framingham Heart Study.* Circulation, 2004. 110(9): p. 1042-1046.

[2] Wallmann, D., et al., *Frequent atrial premature beats predict paroxysmal atrial fibrillation in stroke patients: an opportunity for a new diagnostic strategy.* Stroke, 2007. 38(8): p. 2292-2294.

[3] Rincón, F., et al. *Automated real-time atrial fibrillation detection on a wearable wireless sensor platform*. in *2012 Annual International Conference of the IEEE Engineering in Medicine and Biology Society*. 2012. IEEE.

[4] Padhy, S. and S. Dandapat, *Third-order tensor based analysis of multilead ECG for classification of myocardial infarction.* Biomedical Signal Processing and Control, 2017. 31: p. 71-78.

[5] Padhy, S. and S. Dandapat, *Exploiting multi-lead electrocardiogram correlations using robust third-order tensor decomposition.* Healthcare technology letters, 2015. 2(5): p. 112-117.

[6] Boussé, M., et al. *Irregular heartbeat classification using Kronecker product equations*. in *2017 39th Annual International Conference of the IEEE Engineering in Medicine and Biology Society (EMBC)*. 2017. IEEE.

[7] Goovaerts, G., et al. *Tensor-based detection of T wave alternans in multilead ECG signals*. in *Computing in Cardiology 2014*. 2014. IEEE.

[8] Geirnaert, S., et al. *Tensor-based ECG signal processing applied to atrial fibrillation detection*. in *2018 52nd Asilomar Conference on Signals, Systems, and Computers*. 2018. IEEE.

[9] Beraza, I. and I. Romero, *Comparative study of algorithms for ECG segmentation.* Biomedical Signal Processing and Control, 2017. 34: p. 166-173.

[10] Bolton, R. and L. Westphal, *Preliminary results in display and abnormality recognition of Hilbert transformed ecgs.* Medical and Biological Engineering and Computing, 1981. 19(3): p. 377-384.

[11] Benitez, D., et al., *The use of the Hilbert transform in ECG signal analysis.* Computers in biology and medicine, 2001. 31(5): p. 399-406.

[12] Varghees, V.N. and K. Ramachandran, *A novel heart sound activity detection framework for automated heart sound analysis.* Biomedical Signal Processing and Control, 2014. 13: p. 174-188.

[13] Muda, L., M. Begam, and I. Elamvazuthi, *Voice recognition algorithms using mel frequency cepstral coefficient (MFCC) and dynamic time warping (DTW) techniques.* arXiv preprint arXiv:1003.4083, 2010.

[14] Hunyadi, B., et al., *Tensor decompositions and data fusion in epileptic electroencephalography and functional magnetic resonance imaging data.* Wiley Interdisciplinary Reviews: Data Mining and Knowledge Discovery, 2017. 7(1): p. e1197.

[15] Kruskal, J.B., *Three-way arrays: rank and uniqueness of trilinear decompositions, with application to arithmetic complexity and statistics.* Linear algebra and its applications, 1977. 18(2): p. 95-138.

[16] Sidiropoulos, N.D. and R. Bro, *On the uniqueness of multilinear decomposition of N-way arrays.* Journal of Chemometrics: A Journal of the Chemometrics Society, 2000. 14(3): p. 229-239.

[17] Ribeiro, L.N., A.R. Hidalgo-Munoz, and V. Zarzoso. *Atrial signal extraction in atrial fibrillation electrocardiograms using a tensor decomposition approach*. in *2015 37th Annual International Conference of the IEEE Engineering in Medicine and Biology Society (EMBC)*. 2015. IEEE.